

Effect of Dimensions in Laser Surface Texturing on Cutting Tools

Ahmet ÇALIK

Burdur Mehmet Akif Ersoy University, Faculty of Engineering and Architecture, Department of Mechanical Engineering, 15200, Burdur, Türkiye, E-mail: acalik@mehmetakif.edu.tr

<https://doi.org/10.5755/j02.mech.35761>

1. Introduction

The machining industry constitutes a significant percentage of the manufacturing sector, and materials are brought into a suitable form through machining operations. One of the most important components of machining operations is the cutting tools [1]. Cutting tools remove excess material from the workpiece in chip form, thus bringing the workpiece to the desired geometry [2]-[4].

The high cost of cutting tools used for machining may increase production costs, which could negatively impact a company's profitability. Therefore, companies should conduct R&D activities to develop more efficient and durable cutting tools.

During R&D activities, the durability and efficiency of cutting tools can be improved by using different materials and machining techniques. For instance, the lifespan of cutting tools can be extended using more durable coatings or harder materials. Additionally, the design and geometry of cutting tools can be improved to shorten the machining time and increase the production capacity.

Developing high-quality cutting tools can also help achieve lower surface quality values. For example, sharper cutting edges may be required for cutting tools to obtain a smoother and more even surface. This improves the surface quality of machined parts and shortens production time by requiring fewer machining processes.

In machining operations, a significant amount of friction, cutting force, and heat are generated while removing chips at high speed [5]. This friction, cutting force, and heat cause cutting tools to wear out and increase the contact surface with the workpiece. As a result, lower quality products are produced. Designing cutting tools that are more durable against all these negative effects will increase their lifespan and improve efficiency [6].

Ceramic cutting tools, which can remove a higher number of chips than carbide cutting tools, are widely used in material processing [7]. This is because ceramic cutting tools have high melting points, high hardness, high wear resistance, and chemical stability. However, ceramic cutting tools have a high coefficient of friction. High friction causes the cutting tool to wear out [8]. To reduce all this friction and consequent wear, different approaches have emerged in the industry [9], [10]. One of these approaches is laser patterning.

In recent years, the laser patterning method has been used to improve the tribological values of material surfaces. Initially, it was used in areas such as the production of engine cylinders. Later, the positive results obtained led to the emergence of ideas about the applicability of this process to cutting tools [11], [12]. Engineers researching laser patterning have concluded that this process improves the tribological properties of cutting tools. The patterns applied

on cutting tools facilitate the easy removal of chips during dry cutting, whereas in lubricated and cooled systems, they enable the oil to spread more easily and reduce the friction force [13], [14]. Kolvachenko and colleagues tested the effects of laser patterning on the H-13 material and observed a decrease in friction [15].

To increase wear resistance, reduce friction during machining, distribute lubricating cutting fluid more efficiently over the cutting tool, control heat dissipation through chips, and reduce wear, a surface is created on the cutting tool using laser texturing [16]. K. Zhang and colleagues observed in 2014 that laser texturing positively affected the performance and lifespan of cutting tool edges [12]. In another study, Youqiang Xing and colleagues observed in 2014 that laser texturing applied to a silicon nitride (Si₃N₄) based cutting tool reduced the cutting force and the amount of heat generated during the machining process compared with an untreated cutting tool [9]. Kawasegi et al. tested laser texturing on an A5052 aluminum alloy and found that both cutting force and friction decreased [17]. In a 2020 study, De Zanet and colleagues demonstrated that laser texturing could also be applied to ceramic-based materials [18]. In their 2022 study, Bogdan Antonzewski and his colleague found that lubrication was enhanced and friction was reduced in laser-textured cutting edges [19]. In a 2016 study, Wei et al. observed that the friction coefficient and cutting force generated by a laser-textured cutting tool were lower than those generated by a non-laser-textured tool [20].

In laser patterning processes, the geometry of the designed pattern also affects the performance of the cutting tool. Enver Ali ĞasĞar designed two different patterns with different geometries in his master's thesis and compared them. The results showed that the horizontally patterned tool was more efficient than the vertically patterned tool [21]. In another study on this topic, Youqiang Xing and colleagues compared three pattern geometries. Based on the obtained data, the wavy patterned tool was found to be more efficient than the horizontal and vertical patterned tools [9].

This study focuses on a different approach to increase the efficiency of the laser patterning process that enhances the performance of cutting tools. In this approach, the width of the designed pattern, the gap between the patterns, and the angle between the lines of the pattern were modified to observe the dimensions where most chips were removed and which of these factors had a greater effect on tool performance. The experimental design was created using the Taguchi method and L9 orthogonal array. GG25 cast iron was selected as the material to be machined using the dry cutting method with the turning process. A silicon nitride (Si₃N₄) based cutting tool was used in the experiment. After the experiments, the amount of wear on the cutting tools was examined under a microscope, and the amount of chips lifted by the cutting tool was measured. The patterns

were compared with each other to determine the most efficient combination, and the factor that had the greatest impact on efficiency was identified using the signal-to-noise ratio method.

2. Materials and Methods

2.1. Materials

In this study, GG25 cast iron was used as the material for processing. The mechanical properties and chemical compositions of the material are listed in Tables 1 and 2, respectively. GG25 is an easily machinable material with low production costs. Additionally, it has high strength and wear resistance. For all of these reasons, its use is widespread in industry [22]. Fig. 1 shows the materials used in the experiments.



Fig. 1 Material used in the experiments

Table 1
Mechanical properties of GG25 cast iron [23]

Property	Value
Maximum tensile stress (MPa)	250-350
Brinell hardness (HB)	180-220
Fracture toughness (MPa)	1000

Table 2
Chemical composition of GG25 cast iron [24]

C, %	Fe, %	Mn, %	P, %	Si, %	S, %
3.00-3.25	Rest	0.40-0.70	0.25 maximum	1.85-2.10	0.12 maximum

Silicon nitride (Si₃N₄) based cutting tools were used in this study. The properties of the material are given in Table 3. SiAlON-based cutting tools are commonly used in machining because of their durability in chip removal processes, particularly in materials other than iron. In addition, SiAlON ceramics are high-strength, high-temperature resistant materials with good thermal shock resistance. The main areas of application for these ceramics are machine tool components and metalworking tools [25]. Fig. 2 shows the ceramic content cutting tool used in this study.

Table 3
Properties of SiAlON ceramics [25]

Density, g/cm ³	3.24
Bending Strength, MPa	760
Elastic Modulus, GPa	288
Shear Modulus, GPa	120
Poisson's Ratio	0.25
Hardness, kg/mm ²	1430-1850
Fracture Toughness (MPa.m ^{1/2})	6-7.5



Fig. 2 SiAlON cutting insert (left) and representative mounted view (right)

2.2. Methods

Before conducting the experiments, an experimental design was created using the Taguchi method. The purpose of using the Taguchi method is to perform the minimum number of experiments possible and obtain the most efficient values. The Taguchi method makes it possible to reduce the number of experiments to be performed. As a result, both the cost incurred in the experiments is reduced and the desired result is obtained in a shorter time [22].

In this study, the factors required for using the Taguchi method and their levels were determined as shown in Table 4.

The L9(3³) orthogonal array was selected according to the number of factors and levels given in the table. Table 5 shows the L9(3³) orthogonal array, and the array created with the factors and levels determined in Table 6 is shown in Table 6.

Using the values specified in Table 6. The drawn patterns are shown in Fig. 3 and Fig. 5. Patterns were drawn in different sizes and engraved on the ceramic cutting tools using the i-Mark laser machine. The parameters used during laser engraving are listed in Table 7

The patterns created based on the parameters mentioned above were examined under an Axio Zoom V16 microscope, and the images of these patterns under the microscope are shown in Fig. 3 and Fig. 5.

The widths of the patterns shown in Fig. 3 are 180

Table 4
Factors and levels used in the experiment

Factor	Level 1	Level 2	Level 3
Pattern Width	18 μm	20 μm	25 μm
Pattern Spacing	200 μm	300 μm	400 μm
Pattern Angle	30°	60°	90°

Table 5
L9(3³) orthogonal array

Experiment No	Factor 1	Factor 2	Factor 3
1	Level 1	Level 1	Level 1
2	Level 1	Level 2	Level 2
3	Level 1	Level 3	Level 3
4	Level 2	Level 1	Level 2
5	Level 2	Level 2	Level 3
6	Level 2	Level 3	Level 1
7	Level 3	Level 1	Level 3
8	Level 3	Level 2	Level 1
9	Level 3	Level 3	Level 2

μm . The pattern spacing and angle vary in the pattern models shown in Fig. 3. Specifically, in Fig. 3, a, the pattern spacing is $200\ \mu\text{m}$ and the pattern angle is 30° . In Fig. 3, b, the pattern spacing is $300\ \mu\text{m}$ and the pattern angle is 60° . Finally, in Fig. 3, c, the pattern spacing is $400\ \mu\text{m}$ and the pattern angle is 90° .

Table 6
L9(33) orthogonal array generated with factors and levels

Experiment No	Pattern Width	Spacing between Patterns	Angle of the Patterns
1	$18\ \mu\text{m}$	$200\ \mu\text{m}$	30°
2	$18\ \mu\text{m}$	$300\ \mu\text{m}$	60°
3	$18\ \mu\text{m}$	$400\ \mu\text{m}$	90°
4	$20\ \mu\text{m}$	$200\ \mu\text{m}$	60°
5	$20\ \mu\text{m}$	$300\ \mu\text{m}$	90°
6	$20\ \mu\text{m}$	$400\ \mu\text{m}$	30°
7	$25\ \mu\text{m}$	$200\ \mu\text{m}$	90°
8	$25\ \mu\text{m}$	$300\ \mu\text{m}$	30°
9	$25\ \mu\text{m}$	$400\ \mu\text{m}$	60°

Table 7

Laser pattern parameters

Number of Cycles	Time, ns	Power, %	Frequency, kHz
5	500	100	50

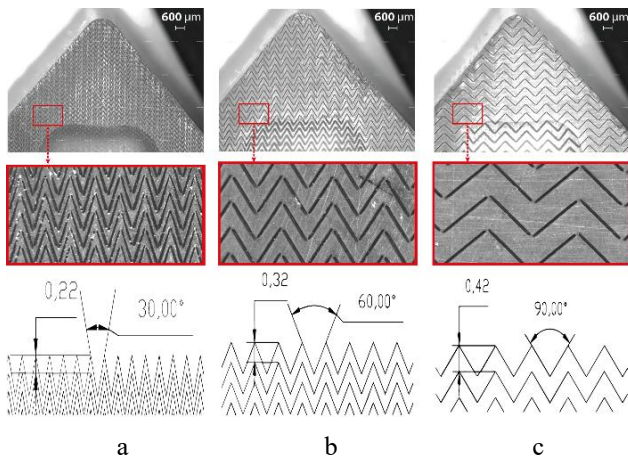


Fig. 3 Laser pattern geometries with $180\ \mu\text{m}$ width applied to cut tool surfaces: a – pattern 1, b – pattern 2, c – pattern 3

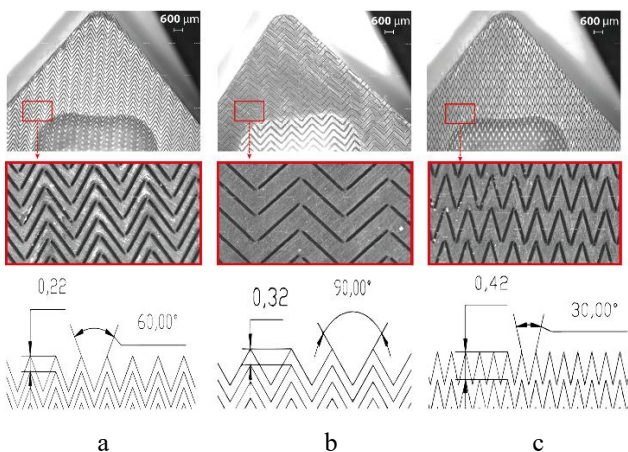


Fig. 4 Laser pattern geometries with $200\ \mu\text{m}$ width applied to cut tool surfaces: a – pattern 4, b – pattern 5, c – pattern 6

The widths of the patterns shown in Fig. 4 are $200\ \mu\text{m}$. The pattern spacing and angle vary in the pattern models shown in Fig. 4. Specifically, in Fig. 4, a, the pattern spacing is $200\ \mu\text{m}$ and the pattern angle is 60° . In Fig. 4, b, the pattern spacing is $300\ \mu\text{m}$ and the pattern angle is 90° . Finally, in Fig. 4, c, the pattern spacing is $400\ \mu\text{m}$ and the pattern angle is 30° .

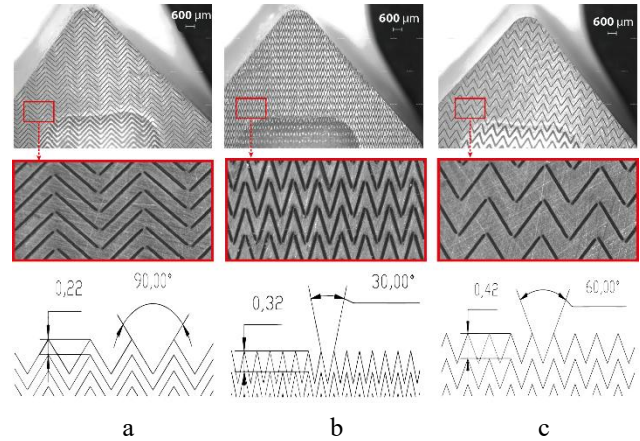


Fig. 5 Laser pattern geometries with $250\ \mu\text{m}$ width applied to cut tool surfaces: a – pattern 7, b – pattern 8, c – pattern 9

The widths of the patterns shown in Fig. 5 are $250\ \mu\text{m}$. The pattern spacing and angle vary in the pattern models shown in Fig. 5. Specifically, in Fig. 5, a, the pattern spacing is $200\ \mu\text{m}$ and the pattern angle is 90° . In Fig. 5, b, the pattern spacing is $300\ \mu\text{m}$ and the pattern angle is 30° . Finally, in Fig. 5, c, the pattern spacing is $400\ \mu\text{m}$ and the pattern angle is 60° .

The performance tests of the ceramic cutting tools produced by laser patterning were carried out on a Doosan Puma V550 CNC lathe machine (Doosan Machine Tools, South Korea). The cutting tools were examined before and after machining using an Axio Zoom V16 stereo zoom microscope (Carl Zeiss, Germany) to measure wear. Laser texturing was performed with an i-Mark industrial laser marking system (XYZ model, ABC Company, Country) using the parameters listed in Table 7. Chemical composition analysis of the GG25 cast iron was carried out using a Foundry-Master Xpert optical emission spectrometer (Hitachi High-Tech, Japan).

During the turning tests, a digital calliper (Mitutoyo, Japan) was used for dimensional checks, and all experiments were conducted under dry cutting conditions without coolant. The spindle speed was set to 600 rpm, and the feed rate was adjusted to $0.3\ \text{mm/rev}$.

The wear on the cutting tools after the turning process was observed, and the amount of wear occurring in different experiments was compared.

The obtained results were compared using the signal-to-noise ratio (S/N Ratio) method, and the most efficient pattern combination and the factor that affects the efficiency the most were determined. The signal-to-noise ratio is a method used to select the best combination of variables in the design [25].

3. Results

The wear amounts of the cutting tools subjected to

laser patterning and processing the GG25 standard material on the lathe machine were examined under a microscope, and the number of GG25 parts from which they were able to remove chips was recorded.

The number of parts in which the cutting tool removes chips is given in Table 9.

Table 9
Number of parts removed by the cutting tool

Side No	Number of Pieces								
	1	2	3	4	5	6	7	8	9
1	15	26	40	40	15	20	8	13	15
2	13	14	15	6	16	24	17	17	8
3	14	12			20	14	18	23	9
4	12	18			9	37	7	17	4
Tot.	54	70	55	46	60	95	50	70	36

In the tool where pattern number 1 was applied, overall free surface and notch wear were observed. The cutting tool could perform chip removal on 54 GG25 parts at the four corners. The wear amount of this cutting tool is shown in Fig. 6, a.

On the tool that processed pattern 2, free surface, notch, and nose wear were observed. It could perform chip removal operation in 70 GG25 parts on four corners. The wear amount of this cutting tool is shown in Fig. 6, b.

The third patterned cutting tool broke at its second corner during the cutting process. Before breakage, nose wear and tool breakage were observed. This tool could perform cutting operations on 55 GG25 parts in two corners. The wear amount of this cutting tool is shown in Fig. 6, c, and the number of parts in which the cutting tool performed the cutting operation until the moment of its breakage is given in Table 9.

The cutting tool with pattern number 4 during its machining operation experienced a fracture in its second corner. Before fracture, nose wear and tool breakage were observed at the edges. This cutting tool performed chip removal operations on 46 GG25 parts with two edges. The wear amount of the cutting tool is shown in Fig. 7, a, and

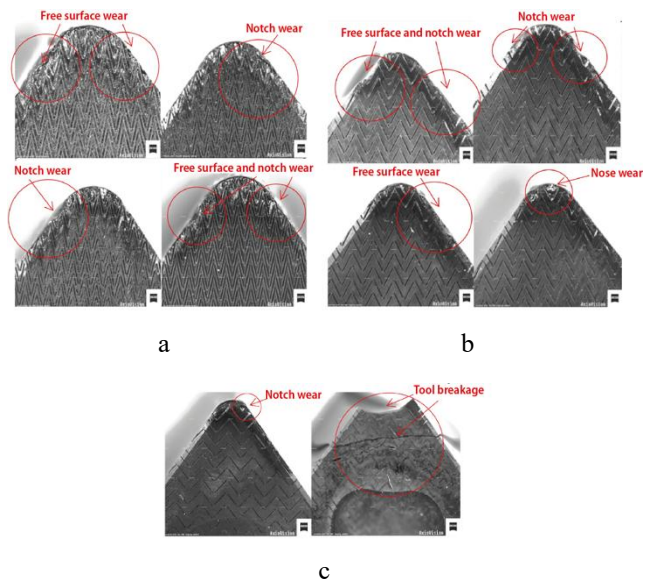


Fig. 6 Wear images of each corner of tools with 180 μm wide laser-etched surface

the number of parts where the cutting tool performed chip removal until the moment of fracture is given in Table 9.

The cutting tool that processed pattern number 5 showed free surface and notch wear. It could perform the chip removal process on 60 GG25 parts with four edges. The amount of wear of this cutting tool is shown in Fig. 7, b, and the number of parts on which the chip removal process was performed is given in Table 9.

On the cutting tool where pattern number 6 is processed, free surface, notch, and nose wear have been observed. The cutting tool performed machining on 95 GG25 parts with four corners. The amount of wear for this cutting tool is shown in Fig. 7, c, and the number of machined parts is given in Table 9.

On the cutting tool where pattern number 7 was processed, free surface wear, nose wear, and tool breakage

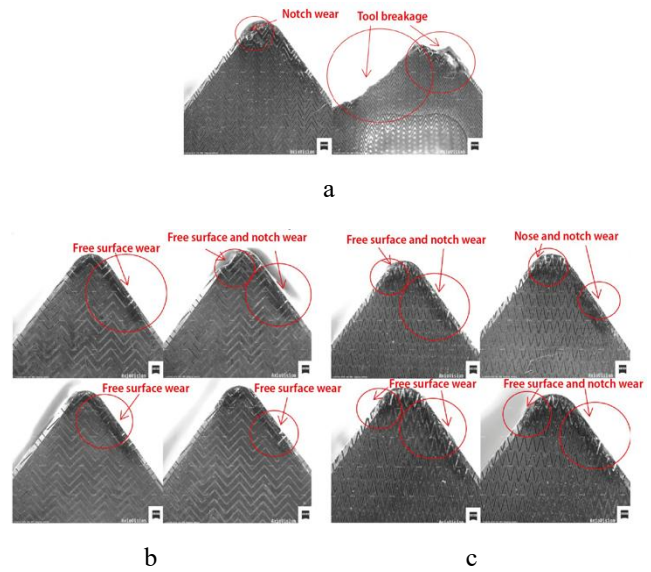


Fig. 7 Wear images of each corner of tools with 200 μm wide laser-etched surface

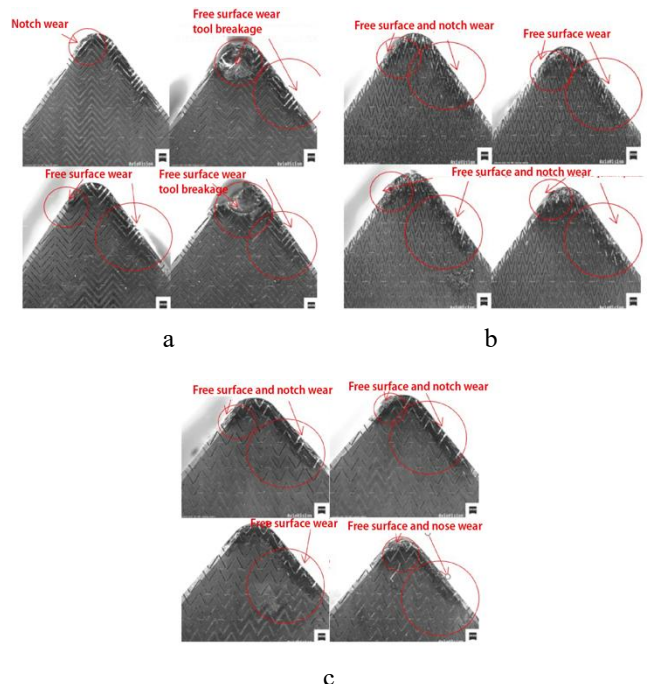


Fig. 8 Wear images of each corner of tools with 250 μm wide laser-etched surface

were observed. The cutting tool performed machining on 50 GG25 parts with four corners. The amount of wear of this cutting tool is shown in Fig. 8, a.

On the cutting tool where pattern number 8 is processed, free surface and notch wear have been observed. The cutting tool performed machining on 70 GG25 parts with four corners. The amount of wear for this cutting tool is shown in Fig. 8, b, and the number of machined parts is given in Table 9.

On the cutting tool where pattern number 9 is processed, free surface, notch, and nose wear have been observed. The cutting tool performed machining on 36 GG25 parts with four corners. The amount of wear of this cutting tool is shown in Fig. 8, c.

The values shown above were obtained from all experiments. These values were entered into the Minitab software, and signal noise processing was applied. After processing, the values shown in Table 10 were obtained.

Table 10

Results in the Minitab

Pattern width	Pattern Spacing	Angle of the Patterns	Number of GG25 Parts	S/N Value
18 μm	200 μm	30°	54	34.6479
18 μm	300 μm	60°	70	36.9020
18 μm	400 μm	90°	55	34.8073
20 μm	200 μm	60°	46	33.2552
20 μm	300 μm	90°	60	35.5630
20 μm	400 μm	30°	95	39.5545
25 μm	200 μm	90°	50	33.9794
25 μm	300 μm	30°	70	36.9020
25 μm	400 μm	60°	36	31.1261

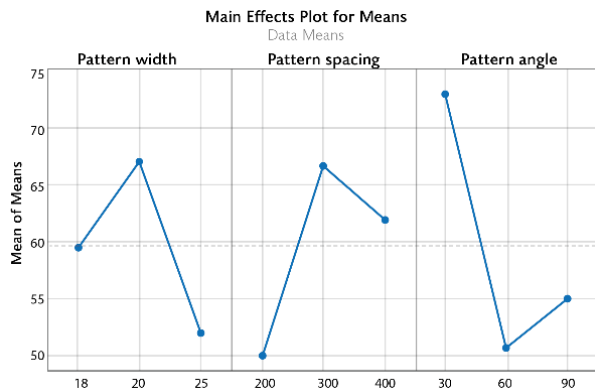


Fig. 10 Minitab-generated main effects plot

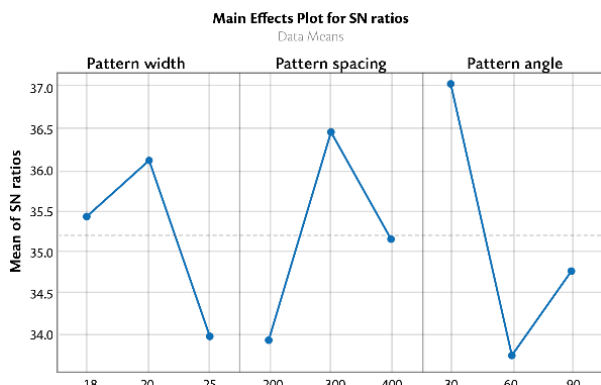


Fig. 11 Signal-to-noise ratio plot obtained in Minitab

According to the results obtained in Figs. 10 and 11, the parameter that has the most impact on performance is the angle of the patterns. Additionally, these values have shown that the pattern width of 20 μm , pattern spacing of 300 μm , and pattern angle of 30° provide the highest performance in the pattern combination that shows the best results.

4. Conclusions

It has been observed that laser patterning applied to ceramic-based cutting tools, designed and applied in different sizes, can be applied to machining on a different number of GG25 parts for each pattern. The tool processed with pattern number 6 achieved the highest performance. The width of pattern number 6 is 20 μm , the distance between the patterns is 400 μm , and the angle of the pattern is 30°.

When the wear on the tools was observed, it was found that in the tools that showed high performance, nose wear was observed, and other types of wear occurred in smaller amounts.

The tools with pattern numbers 3 and 4 broke, but they still managed to perform 40 cuts on GG25 parts at the initial edge, and thus obtained the highest number of cuts. In cases where no breakage occurred, it is believed that four edges can reach the highest total number of cuts.

Other conclusions that can be drawn from this study can be listed as follows:

1. The dimensions used in the design of the pattern during the laser patterning process can have a positive or negative effect on tool performance.

2. The applied process, workpiece, spindle speed, feed rate, whether the process is dry or with coolant, etc. are factors that affect the ideal pattern dimensions.

3. Taking all these factors into account, the pattern shape and dimensions to be designed for each factor may vary. Accordingly, there is no ideal pattern shape or dimensions for all processes. Even a change in the parameters of the laser patterning device can have a significant impact on the performance of the cutting tool.

4. The observation of different types and amounts of wear in each tool subjected to laser patterning demonstrates the effect of this application on wear.

References

1. **Krar S. F.; Gill, A.** 2003. Exploring Advanced Manufacturing Technologies. New York: Industrial Press Inc. 448p.
2. **Kumar, C. S.; Fernandes, F. D.** 2023. Thin-Films for Machining Difficult-to-Cut Materials: Challenges, Applications, and Future Prospects. Boca Raton: CRC Press. 118p.
3. **Kaushish, J. P.** 2010. Manufacturing processes. PHI Learning Pvt. Ltd. 1006 p.
4. **Çevik, E.** 2006. An alternative approach for tool life improvement when turning, Gazi University, MSc Thesis.
5. **Guimarães, B.; Fernandes, C. M.; Figueiredo, D.; Carvalho, O.; Silva, F. S.; Miranda, G.** 2020. Effect of laser surface texturing on the wettability of WC-Co cutting tools, The International Journal of Advanced Manufacturing Technology 111: 1991-1999. <https://doi.org/10.1007/s00170-020-06155-3>.
6. **Sasi, R.; Subbu, S. K.; Palani, I. A.** 2017. Performance of laser surface textured high speed steel cutting tool in

- machining of Al7075-T6 aerospace alloy, *Surface and Coatings Technology* 313: 337-346.
<https://doi.org/10.1016/j.surfcoat.2017.01.118>.
7. **Akkaşoğlu, U.** 2018. Development of ceramic cutting tools with heterogeneous microstructures (Heterojen içyapıya sahip seramik kesici uçların geliştirilmesi), Doctoral dissertation, Eskişehir Anadolu University (Turkey).
 8. **Grigoriev, S. N.; Fedorov, S. V.; Hamdy, K.** 2019. Materials, properties, manufacturing methods and cutting performance of innovative ceramic cutting tools— a review, *Manufacturing Review* 6: 19.
<https://doi.org/10.1051/mfreview/2019016>.
 9. **Xing, Y.; Deng, J.; Zhao, J.; Zhang, G.; Zhang, K.** 2014. Cutting performance and wear mechanism of nanoscale and microscale textured Al₂O₃/TiC ceramic tools in dry cutting of hardened steel, *International Journal of Refractory Metals and Hard Materials* 43: 46-58.
<https://doi.org/10.1016/j.ijrmhm.2013.10.019>.
 10. **Xing, Y.; Deng, J.; Li, S.; Yue, H.; Meng, R.; Gao, P.** 2014. Cutting performance and wear characteristics of Al₂O₃/TiC ceramic cutting tools with WS₂/Zr soft-coatings and nano-textures in dry cutting, *Wear* 318(1-2): 12-26.
<https://doi.org/10.1016/j.wear.2014.06.001>.
 11. **Zhang, K.; Deng, J.; Sun, J.; Jiang, C.; Liu, Y.; Chen, S.** 2015. Effect of micro/nano-scale textures on anti-adhesive wear properties of WC/Co-based TiAlN coated tools in AISI 316 austenitic stainless steel cutting, *Applied Surface Science* 355: 602-614.
<https://doi.org/10.1016/j.apsusc.2015.07.132>.
 12. **Zhang, K.; Deng, J.; Xing, Y.; Li, S.; Gao, H.** 2015. Effect of microscale texture on cutting performance of WC/Co-based TiAlN coated tools under different lubrication conditions, *Applied Surface Science* 326: 107-118.
<https://doi.org/10.1016/j.apsusc.2014.11.059>.
 13. **Fan, L.; Deng, Z.; Gao, X.; He, Y.** 2021. Cutting performance of micro-textured PCBN tool, *Nanotechnology and Precision Engineering (NPE)* 4(2): 023004.
<https://doi.org/10.1063/10.0004372>.
 14. **Da Silva, W. M.; Suarez, M. P.; Machado, A. R.; Costa, H. L.** 2013. Effect of laser surface modification on the micro-abrasive wear resistance of coated cemented carbide tools, *Wear* 302(1-2): 1230-1240.
<https://doi.org/10.1016/j.wear.2013.01.035>.
 15. **Kovalchenko, A.; Ajayi, O.; Erdemir, A.; Fenske, G.; Etsion, R.** 2005. The effect of laser surface texturing on transitions in lubrication regimes during unidirectional sliding contact, *Tribology International* 38(3): 219-225.
<https://doi.org/10.1016/j.triboint.2004.08.004>.
 16. **Duan, R.; Deng, J.; Ai, X.; Liu, Y.; Chen, H.** 2017. Experimental assessment of derivative cutting of micro-textured tools in dry cutting of medium carbon steels, *The International Journal of Advanced Manufacturing Technology* 92: 3531-3540.
<https://doi.org/10.1007/s00170-017-0360-8>.
 17. **Kawasegi, N.; Sugimori, H.; Morimoto, H.; Morita, N.; Hori, I.** 2009. Development of cutting tools with microscale and nanoscale textures to improve frictional behavior, *Precision Engineering* 33(3): 248-254.
<https://doi.org/10.1016/j.precisioneng.2008.07.005>.
 18. **De Zanet, A.; Casalegno, V.; Salvo, M.** 2021. Laser surface texturing of ceramics and ceramic composite materials—A review, *Ceramics International* 47(6): 7307-7320.
<https://doi.org/10.1016/j.ceramint.2020.11.146>.
 19. **Antoszewski B.; Kurp, P.** 2022. Effect of Surface Texture on the Sliding Pair Lubrication Efficiency, *Lubricants* 10(5): 80.
<https://doi.org/10.3390/lubricants10050080>.
 20. **Wei, Y.; Kim, M. R.; Lee, D. W.; Park, C.; Park, S. S.** 2017. Effects of micro textured sapphire tool regarding cutting forces in turning operations, *International Journal of Precision Engineering and Manufacturing-Green Technology* 4: 141-147.
<https://doi.org/10.1007/s40684-017-0017-y>.
 21. **Ğaşğar, E. A.** 2022. Effect of geometry on the insert performance in laser texturing process applied to cement carbide tools (Sement karbür uçlara uygulanan lazer desenleme işleminde geometrinin kesici uç performansına etkileri), Master's Thesis, İzmir Katip Çelebi University (Turkey).
 22. **Düzce R.; Samtaş, G.** 2021. Effect of Cutting Parameters on Cutting Temperature and Optimization in Milling of GG25 Cast Iron, *Manufacturing Technologies and Applications* 2(3): 20-33 (in Turkish).
<https://doi.org/10.52795/mateca.1019186>.
 23. **Uhrynski, A.; Nurkusheva, S.; Ussebayev, M.; Hyla, P.; Bembenek, M.** 2024. A comparative thermal analysis of two workpiece materials of different machinability when turning based on IR thermography, *Journal of Machine Engineering* 24(1): 50-59.
<https://doi.org/10.36897/jme/185359>.
 24. **Martin, D. R.; Moreno, J. R. S.; de Albuquerque Vicente, A.** 2015. Effects of different inoculants on the microstructural characteristics of gray cast iron gg-25, hardness and useful life of tools, *Acta Scientiarum. Technology* 37(4): 355-360.
<https://doi.org/10.4025/actascitechnol.v37i4.27460>.
 25. **Karakuş, N.** 2010. Synthesising and characterization of nitride based ceramic powders from local raw materials, Sakarya University (in Turkish).
 26. **Pignatiello Jr, J. J.** 1988. An Overview of the Strategy and Tactics of Taguchi. *IIE transactions* 20(3): 247-254.
<https://doi.org/10.1080/07408178808966177>.

A. Çalik

EFFECT OF DIMENSIONS IN LASER SURFACE TEXTURING ON CUTTING TOOLS

S u m m a r y

A significant part of the costs the companies that produce with the machining method is the cost of the cutting tool. The high cost and the continuous increase in the competition in the sector have pushed the companies operating in this field to work to extend the life of cutting tools. In this study, laser patterning was applied to the surfaces of silicon nitride-based cutting tools, and the most ideal combination was determined by changing the dimensions of the patterning. Before the laser patterning process, an experimental design was created using the Taguchi method and the L9 orthogonal array. The experiments were carried out on a Do-

san Puma V550 turning machine, and the chip removal process was carried out dry. Material conforming to the GG25 standard is processed on the turning machine. In the experiments, the widths of the patterns, the spaces between the patterns, and the angles between the lines of the patterns were varied. The wear number of the cutting tools was observed using an Axio Zoom V16 microscope. After all these examinations, the data were collected and the results were compared using the signal-to-noise ratio method. With this comparison, it was seen that the most efficient pattern was $20\mu\text{m}-300\mu\text{m}-30^\circ$. In addition, it was determined that the most influential factor on cutting tool performance was the angle of the patterns.

Keywords: laser texturing, Taguchi method, turning, ceramic cutting tool.

Received November 29, 2023
Accepted August 22, 2025



This article is an Open Access article distributed under the terms and conditions of the Creative Commons Attribution 4.0 (CC BY 4.0) License (<http://creativecommons.org/licenses/by/4.0/>).